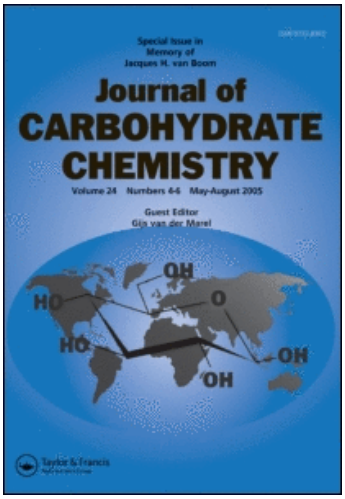

Journal of Carbohydrate Chemistry
Publication details, including instructions for authors and subscription information:
http://www.informaworld.com/smpp/title~content=t713617200

2D- and 3D- Potential Energy Surfaces of β-(1→3)-Linked Disaccharides Calculated with the MM3 Force-Field

Carlos A. Stortz[a]; Alberto S. Cerezo[a]
[a] Departamento de Química Orgánica-CIHIDECAR, Facultad de Ciencias Exactas y Naturales, Universidad de Buenos Aires, Buenos Aires, Argentina

Online publication date: 05 December 2003

To cite this Article Stortz, Carlos A. and Cerezo, Alberto S.(2003) '2D- and 3D- Potential Energy Surfaces of β-(1→3)-Linked Disaccharides Calculated with the MM3 Force-Field', Journal of Carbohydrate Chemistry, 22: 3, 217 — 239
To link to this Article: DOI: 10.1081/CAR-120021702
URL: http://dx.doi.org/10.1081/CAR-120021702

JOURNAL OF CARBOHYDRATE CHEMISTRY
Vol. 22, Nos. 3 & 4, pp. 217–239, 2003

2D- and 3D- Potential Energy Surfaces of β-(1→3)-Linked Disaccharides Calculated with the MM3 Force-Field

Carlos A. Stortz* and Alberto S. Cerezo

Departamento de Química Orgánica-CIHIDECAR, Facultad de Ciencias Exactas y Naturales, Universidad de Buenos Aires, Buenos Aires, Argentina

ABSTRACT

The adiabatic conformational surfaces of sixteen 4′,6′,6-trideoxy-β-D-(1 → 3)-linked disaccharides were obtained using the MM3 force-field. Calculations were carried out on disaccharides with different configurations at C2, C4 and C2′, which are neighbors to the glycosidic linkage, as well as that of the linked carbon (C3). The surfaces were plotted as contour maps and as 2D graphs representing the energy vs. the ψ angle. The resulting maps were similar in each case, indicating that the substituents do not play a major role in the conformational features of these disaccharides. However, the number of minima, the preferred minimum conformation and the flexibility depended on the configurations of the mentioned carbons. Vicinal equatorial substituents tend to decrease the overall flexibility, especially those on C2, although cross over effects were found. The relative stabilities of the minimal energy conformations of the 16 compounds were compared with those of their equivalent α-linked counterparts. Deviations of the predicted increased stabilities of equatorially substituted compounds

*Correspondence: Carlos A. Stortz, Departamento de Química Orgánica-CIHIDECAR, Facultad de Ciencias Exactas y Naturales, Universidad de Buenos Aires, Pabellón 2, 1428 Buenos Aires, Argentina; Fax: 54-11-4576-3346; E-mail: stortz@qo.fcen.uba.ar.

DOI: 10.1081/CAR-120021702
0732-8303 (Print); 1532-2327 (Online)
www.dekker.com

MARCEL DEKKER, INC.
270 Madison Avenue, New York, New York 10016

over axially substituted ones follow a relationship with their configurations, and consequently can serve to formulate predictive trends.

Key Words: Conformational analysis; Disaccharide maps; MM3; Axial; Equatorial.

INTRODUCTION

In order to understand oligosaccharide conformational structures, the features of the glycosidic linkages are usually represented by a Ramachandran-like conformational map.[1–3] These disaccharide contour maps show the energy determined for all mutual orientations of the two monosaccharide residues, expressed by the glycosidic angles ϕ and ψ. Flexible residue analysis was initiated in 1979 and extended in the late 1980s,[4–12] giving rise to the first fully relaxed energy maps of disaccharides. The parameterization of the force-field MM3[13,14] takes into account some problems of carbohydrate modeling[15,16] and consequently has been applied to many different disaccharides as demonstrated by Dowd et al.,[17–20] and others. Another difficulty encountered with disaccharide modeling has its origins in the rotameric complexity of the exocyclic substituents (the ''multiple minimum problem''),[1–3] which has been circumvented using different approaches.[21] French and coworkers[22–24] applied ab initio or hybrid QM/MM3 procedures to map disaccharides, in an attempt to achieve higher accuracy. The use of 2D graphs to replace contour maps as representations of the potential energy surfaces of disaccharides was proposed as a tool to facilitate calculations and help in drawing conclusions.[25]

Rees[26] has predicted that disaccharides with equatorial bonds will be more flexible than those with axial-equatorial bonds, and these in turn even more flexible than those with axial-axial bonds. He also pointed out that bulky equatorial substituents vicinal to the glycosidically linked atoms reduce the flexibility of the linkage more than bulky axial substituents. Work with disaccharide analogs[22] and carrageenan repeating units[27–29] suggested that these assumptions were correct. However, in a recent paper about the potential energy surfaces of α-(1 $\rightarrow$ 3)-linked disaccharides carrying different configurations at C2, C3, C4 and C2′ we have shown that, although equatorial bonds and vicinal axial substituents tend to increase the overall flexibility, these factors can have a cross over effect.[30]

Herein are presented the 2D and 3D potential energy surfaces of sixteen disaccharides of the type 3-*O*-(4,6-dideoxy-β-D-hexopyranosyl)-6-deoxy-β-D-hexopyranose with different configurations at carbons 2, 3, 4 and 2′ (Figure 1), calculated using MM3 at ε = 3. As in the previous paper,[30] comparison with equivalent tetrahydropyran and acyclic derivatives offer an aid to learn about the factors governing the flexibility of these molecules.

METHODS

Calculations were carried out using the molecular mechanics program MM3 (92) (QCPE, Indiana University, USA),[13,14] at a dielectric constant of 3. The MM3

Marcel Dekker, Inc.
270 Madison Avenue, New York, New York 10016

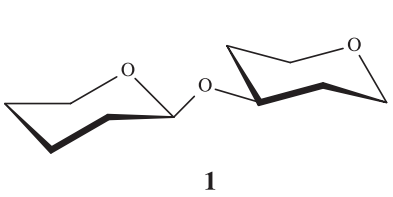

1

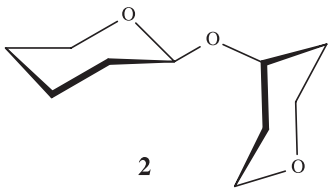

2

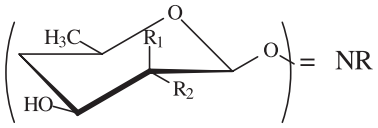

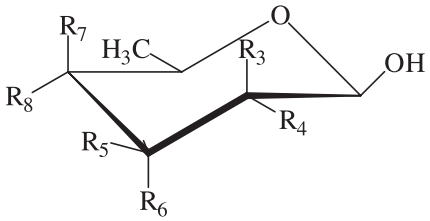

	R_1	R_2	R_3	R_4	R_5	R_6	R_7	R_8	Conf.NR	Conf. R
3	H	OH	H	OH	NR	H	H	OH	D-*xylo*	D-*gluco*
4	H	OH	H	OH	NR	H	OH	H	D-*xylo*	D-*galacto*
5	H	OH	OH	H	NR	H	H	OH	D-*xylo*	D-*manno*
6	H	OH	OH	H	NR	H	OH	H	D-*xylo*	D-*talo*
7	OH	H	H	OH	NR	H	H	OH	D-*lyxo*	D-*gluco*
8	OH	H	H	OH	NR	H	OH	H	D-*lyxo*	D-*galacto*
9	OH	H	OH	H	NR	H	H	OH	D-*lyxo*	D-*manno*
10	OH	H	OH	H	NR	H	OH	H	D-*lyxo*	D-*talo*
11	H	OH	H	OH	H	NR	H	OH	D-*xylo*	D-*allo*
12	H	OH	H	OH	H	NR	OH	H	D-*xylo*	D-*gulo*
13	H	OH	OH	H	H	NR	H	OH	D-*xylo*	D-*altro*
14	H	OH	OH	H	H	NR	OH	H	D-*xylo*	D-*ido*
15	OH	H	H	OH	H	NR	H	OH	D-*lyxo*	D-*allo*
16	OH	H	H	OH	H	NR	OH	H	D-*lyxo*	D-*gulo*
17	OH	H	OH	H	H	NR	H	OH	D-*lyxo*	D-*altro*
18	OH	H	OH	H	H	NR	OH	H	D-*lyxo*	D-*ido*

Figure 1. The β-(1 → 3) linked disaccharides studied in this work: the non-reducing terminals are 4,6-dideoxy-β-D-hexopyranosyl units, while the reducing terminals are 6-deoxy-α-D-hexopyranose units.

routines were modified by changing the maximum atomic movement from 0.25 Å to 0.10 Å.[31] The dihedrals ϕ_H and ψ_H are defined by atoms H1′-C1′-O3-C3 and H3-C3-O3-C1′, respectively. Minimization was carried out by the block diagonal Newton–Raphson procedure for grid points, using the full-matrix procedure for minima and transition states.

MARCEL DEKKER, INC.
270 Madison Avenue, New York, New York 10016

MARCEL DEKKER, INC.
270 Madison Avenue, New York, New York 10016

Table 1. Relative steric and free energies (kcal/mol) and geometries of the minimum-energy conformations in the main trough obtained for the compounds under study, using the MM3 force-field.

	O1′, O3	HO2′, HO2, HO4	Min. **A**			Min. **A′**			Min. **B**			Min. **C**		
			ϕ_H,ψ_H	ΔE	ΔG	ϕ_H,ψ_H	ΔE	ΔG	ϕ_H,ψ_H	ΔE	ΔG	ϕ_H,ψ_H	ΔE	ΔG
1	EE[a]	–	44,42	0.00	0.00	–			34, – 52	0.48	0.54	34,170	3.03	3.67
2	EA	–	42,39	0.00	0.00	–			32, – 50	0.56	0.90	38,173	7.24	7.96
3	EE	EEE	42,24[b]	1.29	0.37	42, – 10	0.00	0.00	–			32,169	3.05	3.39
4	EE	EEA	42,28	0.78	0.00	–			31, – 55	0.00	0.03	37,159	4.21	4.46
5	EE	EAE	38,40	0.00	0.00	–			35, – 35	0.54	0.78	29, – 174	4.14	5.28
6	EE	EAA	39,41	0.20	0.00	–			34, – 58	0.00	0.59	47, – 156	4.06	5.06
7	EE	AEE	45,19[b]	1.29	0.15	46, – 9	0.00	0.00	–			37,165	3.13	3.67
8	EE	AEA	44,28	0.80	0.19	–			34, – 56	0.00	0.00	39,159	4.08	5.02
9	EE	AAE	43,38	0.00	0.00	–			37, – 34	0.17	0.42	37, – 177	3.98	5.27
10	EE	AAA	46,43	0.59	0.00	–			36, – 59	0.00	0.15	49, – 157	4.02	4.81
11	EA	EEE	42,21[b]	0.67	0.50	42, – 2	0.00	0.00	–			33,173	6.92	8.97
12	EA	EEA	41,32	0.00	0.00	45,2	0.19	0.31	21, – 50	1.51	1.91	33,173	6.82	7.84
13	EA	EAE	40,18	0.22	0.00	–			31, – 45	0.00	0.29	37,176	6.58	8.39
14	EA	EAA	43,35	0.00	0.00	–			30, – 51	0.19	0.36	39,174	7.00	7.64
15	EA	AEE	45,26	0.35	0.00	46,–2	0.00	0.15	22, – 49	1.25	1.74	39,174	7.32	9.13
16	EA	AEA	46,37	0.00	0.00	47, – 1	0.31	0.84	27, – 34	1.45	1.72	39,174	7.51	8.20
17	EA	AAE	43,23	0.43	0.19	–			33, – 50	0.00	0.00	40,176	6.70	8.11
18	EA	AAA	43,35	0.00	0.00	–			32, – 51	0.14	0.57	41,174	7.01	7.68
19	–	–	43,39	0.00	0.00	–			33, – 52	0.60	0.99	33,173	2.63	3.51

[a]A = axial substituent, E = equatorial substituent.
[b]These minima appear with higher energy than other points in the adiabatic map.

The automated procedure used to generate the minima[30] was slightly modified: a minimum in the **B** region was searched for each compound. Starting from this conformation, the 243 conformers produced by rotating the exocyclic OH groups were generated and minimized. In some compounds no minimum in the **B** region exists (Table 1), but the minimization procedure encountered a minimum in the **A′** region. The unique minima (3 to 12) with lower energies (less than 1 kcal/mol above the lowest one) were left. The full calculation (243 conformers each) was repeated in the same manner to determine minima in the **A** and **C** regions. The main minimum in each region was used to locate possible minima in the **D–E–F** region. Starting from each of those minima, using both the dihedral drivers 2 and 4, ϕ_H and ψ_H were fully varied using a 20° grid. At each point, energies were calculated after minimization with restraints for these two angles but allowing the other variables to relax. The optimization was terminated when the decrease in energy converged to a value lower than 2 cal/mol. The energy for each grid point was the lowest of any of the unique 15–40 different minima obtained previously. In this way, only the conformation of minimal energy for each ϕ,ψ combination was recorded and thus the conformational adiabatic maps, or potential energy surfaces as function of ϕ and ψ angles were produced. The same procedure, but starting from the **A**, **B** and **C** minima, and restraining only the angle ψ was used to construct the 2D plots.[25] In this case, 10° steps were used. It has been suggested[24] to drive torsion angles in terms of non-hydrogen atoms, given the different motions of the three atoms during driven rotation and the inaccuracy of hydrogen atom positions in diffraction studies. However, in order to keep up with our previous studies[25,27–30] we continued driving in terms of hydrogen atoms. For compounds in which flipping of the chair was assumed feasible (e.g., *ido* configuration), special care was taken to include in the map only conformers with the original chair conformations ($^4C_1$). Free energies were calculated from the vibrational analysis of the minima, with no special treatment for the low-frequency vibrations:[32] i.e., the effect of frequencies equal or lower than 20 cm^{-1} was added to the MM3 output values (which do not include those frequencies) of vibrational enthalpies and entropies.

The absolute flexibility was calculated as described by Koca et al.[15,16] The formulas for calculating the absolute flexibility and partition function with respect to both angles or just to the ψ angle are described elsewhere.[25,30] The percentage of allowed surfaces was calculated as a quotient of the number of points below certain energy and 324 (the total number of points in a 20° × 20° grid). From the contour maps, the average energies[17–19] for each compound were calculated as:

$$E_{av} = \frac{\sum_{i=1}^{324} E_i \cdot e^{-Ei/RT}}{\sum_{i=1}^{324} e^{-Ei/RT}}$$

where E_i are the energies at each grid point, R is the gas constant, and T, the absolute temperature (set to 298.16 K).

MARCEL DEKKER, INC.
270 Madison Avenue, New York, New York 10016

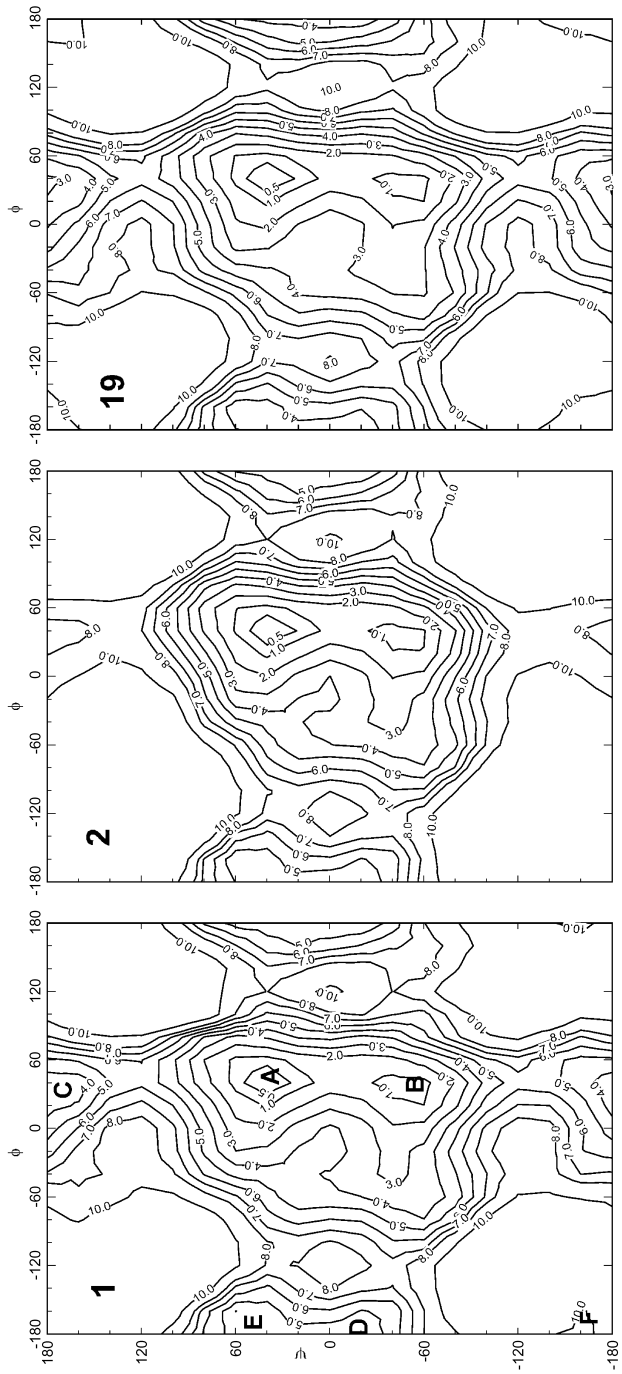

Figure 2. Contour maps of compounds **1**, **2** and **19**, generated using MM3. Iso-energy contour lines are graduated at 0.5, 1, 2, 3, 4, 5, 6, 7, 8 and 10 kcal/mol increments above the global minimum.

Marcel Dekker, Inc.
270 Madison Avenue, New York, New York 10016

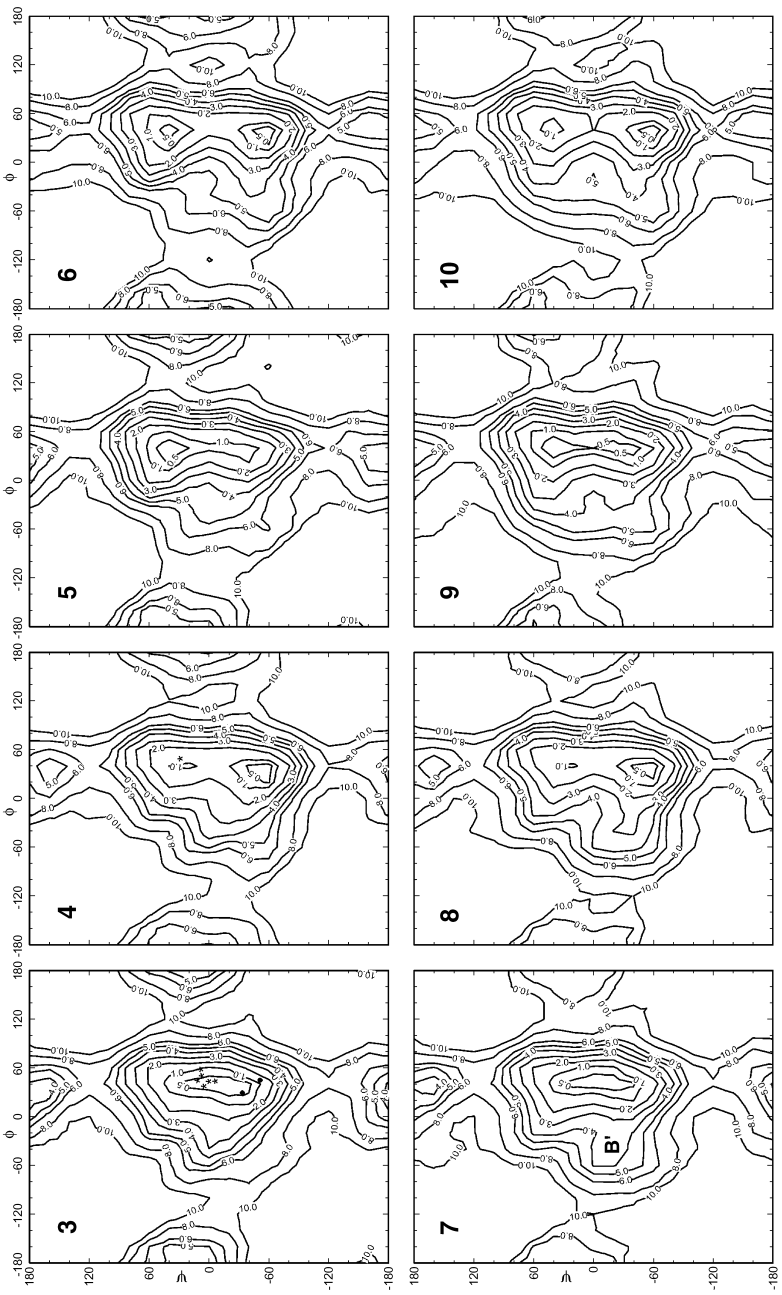

Figure 3. Contour maps of compounds **3–10**, generated using MM3. Iso-energy contour lines are graduated at 0.5, 1, 2, 3, 4, 5, 6, 8 and 10 kcal/mol increments above the global minimum. On the map of **3**, the stars and circles represent the position of reported crystal structures[33–38] for laminarabiose derivatives with acetylated and free hydroxyl groups, respectively. The star on the map of **4** represents the position of a reported crystal structure.[39]

MARCEL DEKKER, INC.
270 Madison Avenue, New York, New York 10016

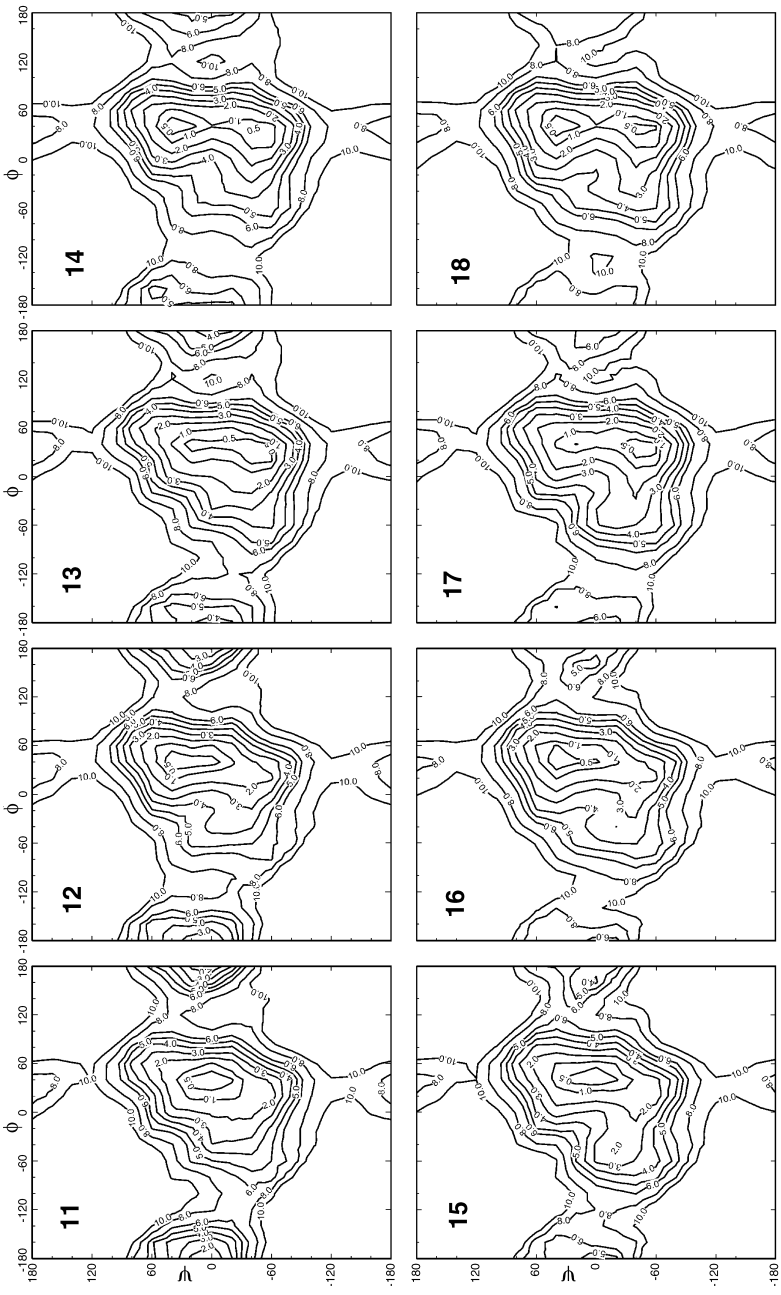

Figure 4. Contour maps of compounds **11–18**, generated using MM3. Iso-energy contour lines are graduated at 0.5, 1, 2, 3, 4, 5, 6, 8 and 10 kcal/mol increments above the global minimum.

Marcel Dekker, Inc.
270 Madison Avenue, New York, New York 10016

RESULTS

The conformational maps of the sixteen 4′,6′,6-trideoxy-β-D-(1 → 3)-linked disaccharides shown in Figure 1 were calculated using MM3 at a dielectric constant of 3. For comparison purposes, the same analysis was carried out with **1**, the analog of **3–10** without exocyclic substituents (diequatorially linked 4-(tetrahydropyran-2-yloxy)tetrahydropyran), and **2**, the corresponding equatorially-axially linked analog of **11–18**. Data for the acyclic analog (*S*)-1-isopropoxyethanol (**19**), adapted from that of its enantiomer[30] is also included.

The resulting contour maps are shown in Figures 2 (compounds **1**, **2** and **19**), 3 (compounds **3–10**) and 4 (compounds **11–18**), while the corresponding 2D plots appear in Figures 5 (**1**, **3–6** and **11–15**) and 6 (**2**, **7–10** and **15–18**). The energy and geometry data on the minima are shown in Tables 1 (minima on the main trough) and 2 (other minima). X-ray crystallographic studies reported the solid-state structures for several laminarabiose derivatives[33–38] with the configuration of **3**, and of a galactobiose derivative[39] with the configuration of **4**. Figure 3 also shows their

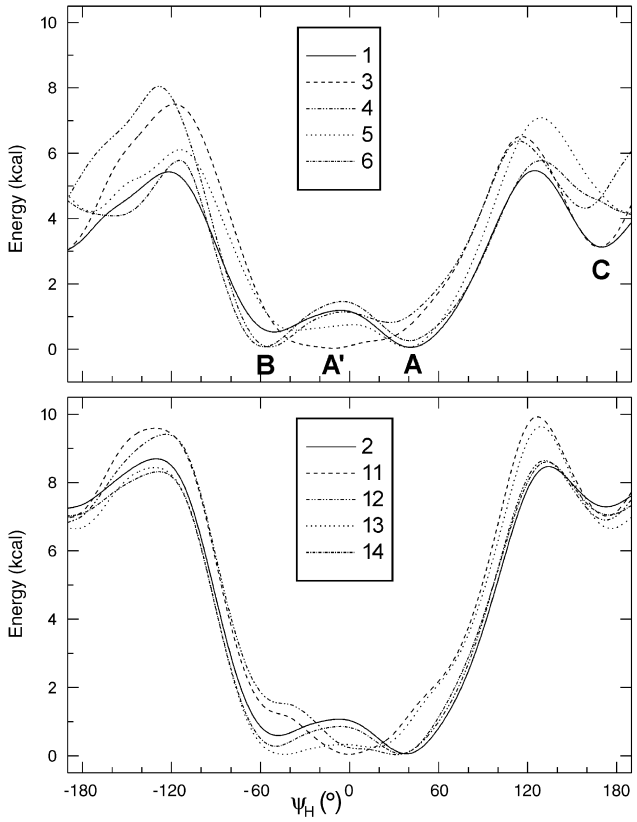

Figure 5. Relaxed MM3 surface (2D plot) for compounds **1–6** and **11–14**.

MARCEL DEKKER, INC.
270 Madison Avenue, New York, New York 10016

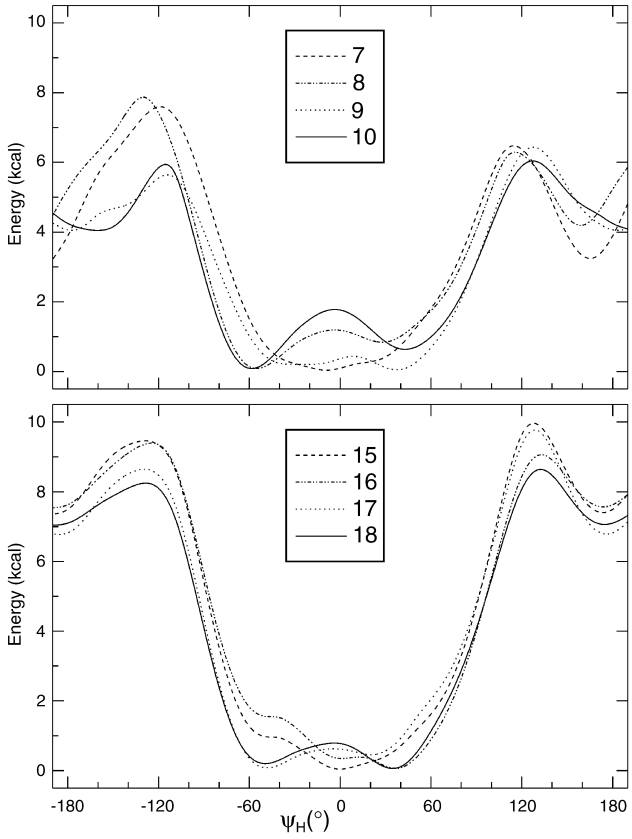

Figure 6. Relaxed MM3 surface (2D plot) for compounds **7–10** and **15–18**.

torsional angles. All the contour maps show similar shapes. The main trough has a ϕ_H angle around that predicted by the *exo*-anomeric effect (ca. 40°). A well within this trough has usually two minima, called **A** and **B** (ψ_H g^+ and g^-, respectively) with similar energies (Table 1). However, in some compounds a minimum called **A′**, with eclipsed ψ_H replaces minimum **B** or appears as a third minimum in that region. Minimum **A** always appears, but in compounds where minimum **A′** appears instead of minimum **B**, minimum **A** is not part of the adiabatic map, which then only shows one minimum (**A′**) in the main region (Figures 2–6). Minimum **C** (ψ_H *t*) is only important (less than 5 kcal/mol above the global minimum) for compounds **3–10** and **1** in which the glycosidic linkage to O3 is equatorial, or in the acyclic compound **19**. The ''side of the map'' region,[40] also complying with the *exo*-anomeric effect (ϕ_H *ca.* 180°) is quite more favorable than in α-linked compounds.[30] Again, three more minima appear in this region for most of the compounds. Their ψ values resemble those encountered for the **A**, **B** and **C** minima (Table 2). In some compounds (**7**, **15** and **17**), a minimum with ϕ,ψ around $-40°$, $-20°$ (in a flat region, **B′**) has been found. Figures 7 and 8 show molecular

Table 2. Relative steric and free energies (kcal/mol) and geometries of the minimum-energy conformations outside the main trough obtained for the compounds studied using the MM3 force-field.

	O1′, O3	HO2′, HO2, HO4	Min. **B′**			Min. **D**			Min. **E**			Min. **F**		
			ϕ_H,ψ_H	ΔE	ΔG	ϕ_H,ψ_H	ΔE	ΔG	ϕ_H,ψ_H	ΔE	ΔG	ϕ_H,ψ_H	ΔE	ΔG
1	EE[a]	–	–			– 178, – 15	3.93	4.61	– 165,56	3.80	4.79	– 173, – 159	8.99	10.65
2	EA	–	–			– 178, – 14	3.91	4.57	– 163,55	3.96	5.01	170,162	15.52	16.95
3	EE	EEE	–			– 178,10	3.79	4.90	– 168,41	4.35	5.01	– 175, – 158	9.16	10.85
4	EE	EEA	–			178,3	4.88	4.75	– 170,46	5.03	5.71	– 176, – 178	10.15	12.07
5	EE	EAE	–			180,10	4.43	5.29	– 168,60	3.76	5.06	– 177, – 145	8.90	11.53
6	EE	EAA	–			176, – 8	4.58	4.97	– 170,62	3.98	5.16	168,155	11.83	13.39
7	EE	AEE	– 47, – 13	3.35	3.17	166,8	5.73	6.53	– 171,47	5.61	6.43	– 180, – 157	11.55	12.94
8	EE	AEA	–			170,8	6.04	6.30	– 172,48	5.87	6.77	– 178, – 170	13.21	14.45
9	EE	AAE	–			163,23	6.08	6.41	– 171,58	4.46	5.84	173, – 144	10.83	13.67
10	EE	AAA	–			178, – 13	6.21	6.31	– 172,60	5.02	5.80	143,168	13.52	14.02
11	EA	EEE	–			– 178,4	0.97	2.85	–			–		
12	EA	EEA	–			179,5	1.90	3.10	–			168,165	16.04	18.03
13	EA	EAE	–			175,4	3.44	3.89	– 164,42	4.56	6.20	178, – 164	16.17	18.52
14	EA	EAA	–			172,11	4.57	4.70	– 169,51	4.57	5.02	168,163	15.19	16.70
15	EA	AEE	– 46, – 19	1.82	2.13	165,5	3.36	5.25	– 165,43	5.06	6.46	152,169	20.00	22.66
16	EA	AEA	–			162,7	4.22	5.65	– 166,53	6.08	6.81	158,164	19.30	21.01
17	EA	AAE	– 37, – 32	2.44	2.17	171,3	5.20	5.37	– 165,44	5.88	6.90	162, – 160	22.28	21.97
18	EA	AAA	–			176, – 11	6.08	6.50	– 167,55	5.78	6.82	– 180,162	18.82	19.50
19	–	–	–			– 177, – 15	3.21	3.90	– 164,54	3.08	4.24	– 170, – 164	7.71	9.56

[a]A = axial substituent, E = equatorial substituent.

MARCEL DEKKER, INC.
270 Madison Avenue, New York, New York 10016

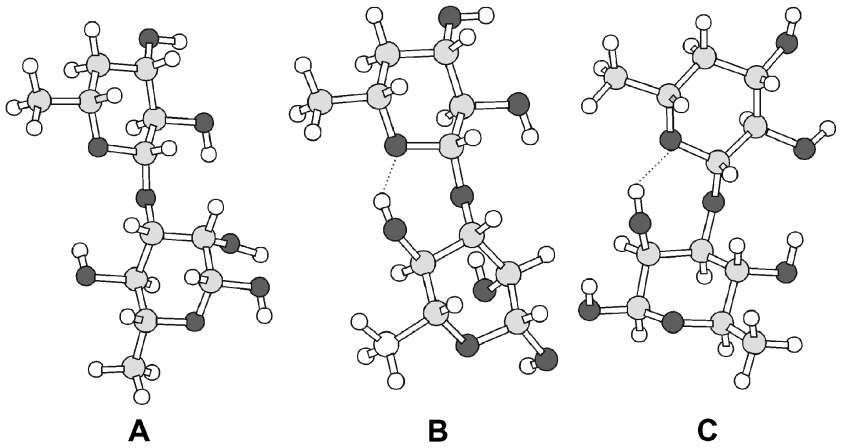

Figure 7. Molecular drawings of the minimum-energy conformers of compound **5** in the **A–C** regions. Hydrogen bond arrangements are shown with dotted lines.

drawings for the minimum-energy conformations of compound **5** in each of the six regions. Table 3 shows the major hydrogen-bond arrangements for the compounds under study.

Flexibility calculations (conformational partition functions and absolute flexibilities, considering both 2D and 3D maps, and contour map allowed surfaces) for these compounds are shown on Table 4. Table 5 shows the relative energies of each of the sixteen disaccharides (for the minimal conformations and average) under study, and comparison with their α-linked counterparts.

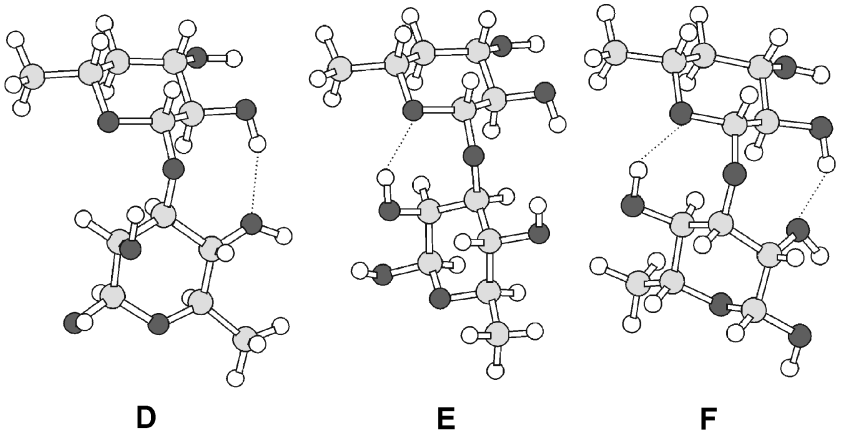

Figure 8. Molecular drawings of the minimum-energy conformers of compound **5** in the **D–F** regions. Hydrogen bond arrangements are shown with dotted lines.

Table 3. Major hydrogen-bond arrangements (E_{HB} > 0.6 kcal/mol) in each minima for the sixteen compounds studied using the MM3 force-field.

	O1′, O3	HO2′, HO2, HO4	H(O)2-O5′	H(O)4-O5′	H(O)2′-O2 or H(O)2-O2′	H(O)2′-O4	H(O)4-O2 or H(O)2-O4	None
3	EE[a]	EEE	**D**, **E**	**A′**, **F**		**D**		**A**,**C**
4	EE	EEA	**C**, **D**, **E**	**B**, **F**	**F**			**A**
5	EE	EAE	**C**, **E**	**B**, **F**	**F**	**D**		**A**
6	EE	EAA	**C**, **E**	**B**, **F**			**A**, **B**, **C**, **D**, **E**, **F**	
7	EE	AEE	**C**, **D**, **E**	**A′**, **F**	**B′**	**D**		**A**
8	EE	AEA	**C**, **D**, **E**	**B**, **F**				**A**
9	EE	AAE	**C**	**B**, **F**	**F**			**A**, **D**, **E**
10	EE	AAA	**C**	**B**, **F**	**F**		**A**, **B**, **C**, **D**, **E**, **F**	
11	EA	EEE	**A′**	**C**, **D**	**D**			**A**
12	EA	EEA	**A′**		**D**			**A**, **B**, **C**, **E**
13	EA	EAE		**C**, **D**, **E**		**F**		**A**, **B**
14	EA	EAA					**A**, **B**, **D**, **E**	**C**, **F**
15	EA	AEE	**A′**	**C**, **D**, **E**	**D**	**B′**, **F**		**A**, **B**
16	EA	AEA	**A′**, **B**		**D**			**A**, **C**, **E**, **F**
17	EA	AAE		**C**, **D**, **E**				**A**, **B**, **B′**, **F**
18	EA	AAA					**A**, **B**, **D**, **E**	**C**, **F**

[a]A = axial substituent, E = equatorial substituent.

MARCEL DEKKER, INC.
270 Madison Avenue, New York, New York 10016

MARCEL DEKKER, INC.
270 Madison Avenue, New York, New York 10016

Table 4. Corrected partition functions q and absolute flexibilities Φ (for two- and tridimensional plots) and percentages of the contour map surfaces below each energy range (''allowed conformations'') for the 19 compounds studied using the MM3 force-field. For the sake of comparison, selected data for their α-linked counterparts[30] is also included in the Table.

			β-linked compounds									α-linked compounds		
									% Allowed					
	O3	HO2′, HO2, HO4	q_ψ (deg)	$q_{\phi,\psi}$ (deg^2)	$q_{\phi,\psi}/q_\psi$	Φ_ψ ($\times 10^4$)	$\Phi_{\phi,\psi}$ ($\times 10^4$)	$\Phi_{\phi,\psi}/\Phi_\psi$	2 kcal	5 kcal	10 kcal	$q_{\phi,\psi}$ (deg^2)	$\Phi_{\phi,\psi}$ ($\times 10^4$)	% Allowed to 2 kcal
1	E[a]	–	57	1760	31	167	96	0.58	5.9	27	68	1650	72	4.9
2	A	–	53	1700	32	195	117	0.60	5.9	22	55	1390	78	4.9
3	E	EEE	71	2120	30	64	34	0.52	5.6	18	49	960	82	3.7
4	E	EEA	45	1400	31	188	119	0.63	5.6	16	51	1230	13	4.3
5	E	EAE	57	1780	31	266	158	0.60	5.9	18	52	2670	243	7.1
6	E	EAA	59	1830	31	120	73	0.61	6.2	20	60	1530	57	5.2
7	E	AEE	66	1900	29	67	35	0.53	5.2	17	50	730	16	2.5
8	E	AEA	44	1330	30	174	109	0.62	5.6	17	52	1430	18	4.6
9	E	AAE	82	2400	29	437	253	0.58	6.5	20	58	1830	81	6.2
10	E	AAA	45	1290	29	68	42	0.62	4.9	20	58	1890	86	5.6
11	A	EEE	49	1780	36	ca.0[b]	ca. 0[b]	2.64	6.2	18	45	1650	105	5.2
12	A	EEA	59	1760	30	279	157	0.56	5.6	19	50	2610	404	5.9
13	A	EAE	74	2500	34	520	335	0.65	6.8	19	48	850	19	3.4
14	A	EAA	63	1910	30	272	166	0.61	5.9	18	51	1230	64	4.3
15	A	AEE	57	1820	32	17[b]	14[b]	0.85	5.9	20	46	2010	113	5.6
16	A	AEA	54	1690	31	226	147	0.65	5.2	18	48	2340	364	5.9
17	A	AAE	58	1890	32	381	254	0.67	5.6	18	47	1160	28	4.0
18	A	AAA	68	2150	31	299	184	0.62	6.2	18	53	1560	104	4.9
19	–	–	56	1770	32	165	94	0.57	6.2	30	71	1770	94	6.2

[a]A = axial substituent, E = equatorial substituent.
[b]Transition states in the main minima region were not encountered.

Table 5. Relative steric (ΔE_{min}) and free energies (ΔG_{min}) for the minimum energy conformer, and average steric energies (ΔE_{av}) of each of the disaccharides under study and their α-linked counterparts,[30] using the MM3 force-field. All energies are expressed in kcal/mol.

		HO2′, HO2, HO4	β-linked			α-linked		
	O3		ΔE_{min}	ΔE_{av}	ΔG_{min}	ΔE_{min}	ΔE_{av}	ΔG_{min}
3	E[a]	EEE	0.00	0.00	0.00	1.12	1.47	1.89
4	E	EEA	0.89	1.17	1.43	1.90	2.04	2.22
5	E	EAE	1.22	1.36	1.19	2.97	2.98	3.36
6	E	EAA	2.02	2.18	2.87	2.82	3.00	3.87
7	E	AEE	1.61	1.65	2.03	1.75	2.02	2.63
8	E	AEA	2.58	2.88	3.26	2.87	3.00	3.39
9	E	AAE	3.25	3.27	3.47	3.54	3.66	4.04
10	E	AAA	3.48	3.77	4.95	3.77	3.93	4.64
11	A	EEE	3.55	3.73	3.31	3.99	4.08	4.78
12	A	EEA	4.21	4.30	4.06	4.71	4.63	4.66
13	A	EAE	3.70	3.73	3.43	4.12	4.28	4.51
14	A	EAA	2.75	2.88	3.27	3.36	3.57	4.24
15	A	AEE	5.34	5.52	5.35	5.12	5.13	5.69
16	A	AEA	5.71	5.86	5.87	5.58	5.57	5.90
17	A	AAE	5.25	5.45	5.77	4.74	4.94	5.20
18	A	AAA	4.41	4.52	5.27	4.13	4.35	5.09

[a]A = axial substituent, E = equatorial substituent.

DISCUSSION

The potential energy surfaces of many disaccharides were analyzed with the MM3 force-field.[17–21] A systematic work has been carried out for α-(1 → 3)-linked disaccharides composed of two D-hexose residues, in an attempt to correlate the potential surfaces with the configurations of the carbons bearing hydroxyl groups vicinal to the glycosidic linkage, as well as that of the glycosidic linkage itself.[30] In that work, to facilitate the calculations, and to achieve a more reliable adiabaticity of the map, hydroxyl groups located far from the glycosidic linkage have been eliminated. In this work, a similar approach was carried out with β-(1 → 3) linked disaccharides. As shown previously, the general conclusions may also be extended to the fully hydroxylated disaccharides.[30]

Shape of the Potential Surfaces

The contour maps show the typical features of those of β-linked disaccharides.[17–20,40] The analogs **1** and **2** (Figure 2) show a main trough, centered at a more or less fixed ϕ_H angle (between 0° and 60°), containing the three main minima, each of which exhibits a clearly different ψ_H angle. A second trough appears at the other ϕ angle favored by the *exo*-anomeric effect (ϕ_H ca. 180°, ''side-of the-map'' minima[40]), and also encompasses three minima, each with ψ values similar to those in the main trough. This region has very high energies in disaccharides with axial

glycosidic linkage,[22–24,30,40] and is ''connected'' to the main trough by a crossing channel around ψ_H 0°, with barriers between the troughs around 8 kcal/mol (negative ϕ_H) and 10 kcal/mol (positive ϕ_H). Surprisingly, the same shape of the map and geometrical features of the minima (Table 1, Figure 2) was observed for the simple acyclic hemiacetal **19**, indicating that the main conformational features of the map are dictated by the C—O—C bond, and less by the substituents. The configuration of C3 defines the depth of the **C** region: this minimum is attainable for equatorial linkages on C3, but carries high energies when this linkage is axial. This is clearly observed in the contour maps (cf **1** and **2**, Figure 2). However, human perception allows recognizing this fact even better in the 2D plots[25] (Figure 5). The introduction of hydroxyl and methyl groups on the tetrahydropyran derivatives does not change the main features of the maps: the contour maps for **3–10** are very similar to that of **1**, while those for **11–18** are like that of **2** (Figures 2-6). For some compounds (**7**, **15** and **17**), another minimum (**B′**, Table 2) in a plateau region appears. An equivalent minimum, called ''non-*exo*-anomeric'',[40] was also detected sometimes for α-linked compounds (on the upper-right side of the maps),[30] and reported to be non-systematic.[18] In the present work, this minimum appears only in compounds with axial O2′ and equatorial O4. Its presence may be related to the possibility of engaging in a hydrogen bond (Table 3). In the main trough, usually two main minima (**A** and **B**) appear, with very close relative energies. Those with the reducing moiety with D-*manno*, D-*gulo* or D-*ido* configuration have **A** as the main minimum, as occurs with the non-substituted analogs **1** and **2** (and the acyclic **19**), whereas those carrying a reducing moiety with D-*galacto*, D-*talo* or D-*altro* configuration show **B** as the main minimum. On the other hand, those compounds with both O2 and O4 equatorial (D-*gluco* and D-*allo* configurations) exhibit a global minimum in a region intermediate between **A** and **B** (**A′**, ψ_H ca. 0°, Table 1, see Figures 5 and 6). Furthermore, in three of these compounds (**3**, **7** and **11**), the minimum **B** does not exist, while the **A** minimum appears, but with an energy above that of the adiabatic map. This fact confers to these contour maps (Figures 3 and 4) and 2D plots (Figures 5 and 6) a differentiated shape, with only one minimum in the main region. Minimum **A′** also appears in compounds having the reducing moiety with D-*gulo* configuration, giving a three-minimum well. However, in these compounds (**12** and **16**), the **B** minima carry higher energies (Table 1). The effects of the substituents on the relative energies of the main minima are interrelated, but exhibit sharp correlations with their orientations, even more comprehensible than for α-linked compounds:[30] the concurrence of equatorial O2 and O4 (irregardless of the orientation of O3) favors minimum **A′**. For the remaining twelve compounds, a combination of O3 and O4 either axial or equatorial favors minimum **A**, while combinations with different configurations at O3 and O4 lead to **B** as the global minimum. Consequently, with the exception of compounds with equatorial HO2 and HO4, the configurations of HO2 and HO2′ are not important for defining the relative energies of the main minima. These effects can neither be explained at all on grounds of hydrogen-bonding, (as all the minima are similarly stabilized in most compounds, Table 3) nor by the measurement of H1′-H2 distances, which are related to the configurations of O2 and O3, but not on that of O4, which was found to be crucial to the determination of the global minimum. The crystal structures reported[33–38] for compounds with the configuration of **3** (D-*gluco*) with acetylated hydroxyl groups have their glycosidic torsion angles in the **A′** region, in agreement with the results of this work. The same fact occurs on an acetylated

Marcel Dekker, Inc.
270 Madison Avenue, New York, New York 10016

analog[39] of **4**, which, in agreement with the present calculation, shows a geometry within the **B** region (Figure 3). On the other hand, analogs of **3** with free hydroxyl groups[33,36] have a crystal structure in the **B** region, which fails to appear in the present calculation.

The relative energies of the minima in the ''side of the map'' region (ϕ_H ca. 180°) are variable (1–6 kcal/mol, Table 2). In compounds with axial O3, minimum **D** carries less energy than minimum **E** in most cases, though their energies are levelled for compounds with axial O2 and O4 (**14** and **18**) or without substituents (**2**). On the other hand, in compounds with equatorial O3, minimum **E** appears stabilized in compounds with axial O2 (**5**, **6**, **9** and **10**), and levelled with **D** or unfavored for the remaining compounds (**1**, **3**, **4**, **7** and **8**). The **D–E** area is relatively favored in compounds **11** and **12** (with respect to the **A–B** region), with an axial O3 and equatorial O2′ and O2, while it appears unfavored in compounds **7**, **8**, **10**, **17** and **18**. Only the cases of **10** and **18** may be explained on grounds of hydrogen bonding.

It is worthy of note that, in the same way that the map of **19** is identical to that of its enantiomer[30] after a 180° rotation, the maps of the β-linked disaccharides (Figures 2 Figures 3 Figures 4) have a similar relationship with equivalent α-linked disaccharides,[30] with the main trough shifted from $\phi_H \approx 40°$ in β-linked compounds to $\approx -40°$ in α-linked compounds, and the non *exo*-anomeric minima with both ϕ_H and ψ_H g^- in β-linked compounds and g^+ in α-linked compounds. As occurred with α-linked compounds,[30] the presence or absence of bulky substituents does not have a major effect on the general shape of the maps and/or the flexibilities. The acyclic model like **19** gives a map and a flexibility with similar characteristics to those of **1–18**. This fact emphasizes again the prime role of the torsional energies in determining energy surfaces, and the small variations produced by the presence and configuration of the substituents.

Free Energy Calculations

Conformational entropy does not need to be uniformly distributed:[28,30,32] it should be expected that strongly hydrogen-bonded conformers will have a reduced mobility, with an unfavorable entropic contribution, thus leading to relatively higher free energies.[24,30] Table 1 shows that considering free energies, the energies of the **A**′ and/or **B** minima appear increased relative to those of the **A** minima in all cases. This agrees with the calculated hydrogen-bond arrangements, usually not occurring in the **A** minima, and more likely to occur in minima **A**′ and **B** (Table 3). Free-energy calculations also tend to give higher values of relative energies for the remaining minima (**C**, **D**, **E** and **F**), possibly by an entropic effect (their wells are less deep, Figures 2–4). However, in some cases this effect is negligible (Tables 1 and 2).

Flexibilities

Different ways of measuring the flexibility of the glycosidic linkage have been devised.[30] The partition function or probability volume[22–24,27–30] is highly dependent on the size of the regions of the map with very low energy and thus, highly influenced by the entropy of the global minimum. The absolute flexibility[15,16,30] gives an indication of the conformational interconversions of the lower-

MARCEL DEKKER, INC.
270 Madison Avenue, New York, New York 10016

energy minima, and is very sensitive to the height of the lower potential barriers. Another parameter, used earlier as a semiquantitative measurement in rigid residue analysis,[41] can be defined in terms of ''allowable surfaces'', offering the notion of the percentage of the surface with an energy below a certain value. It is also related with the entropy of the global minimum, but in a more linear fashion than the partition function. Table 4 shows the results of calculating these parameters for the compounds under study. The partition function and absolute flexibilities were also calculated for the 2D plot: the predicted correlation between both values seems to hold,[25] as shown by the more or less constant values of both ratios (Table 4). This is expected considering the high energies of minima carrying a ϕ angle sharply different from that of the global minimum.

The prediction that equatorially linked disaccharides are more flexible than those that carry at least an axial bond[26] was shown to be true in several cases.[22–24,27–30] Comparison of the compounds under study with their equivalent α-linked counterparts[30] (which carried one more axial linkage) also follows this trend. The allowed surfaces of the β-linked compounds to 10 kcal/mol are larger for the 18 compounds under study, and so occurs with most of those considered to 5 kcal/mol. The partition functions, absolute flexibilities and allowed surfaces to 2 kcal/mol of α-linked compounds were larger only for the equivalents of **5**, **10**, **12** and **16** (Table 4). Besides, increased partition functions were encountered for the α-linked equivalents of **8** and **15**, and increased absolute flexibilities for the equivalents of **3**, **11** and **15**. The absolute flexibilities of the last three compounds are very low, given the fact that no transition states are found within the main well (Table 4). Within the β-linked compounds under study in the present work, the inspection of allowable surfaces to 10 kcal/mol indicate clearly that diequatorially linked compounds (or acyclic **19**) are more flexible, as expected considering the contribution of the **C** region. Within each group, the presence of diaxial substituents on O2 and O4 increase the flexibility. The allowable surfaces to 5 kcal/mol are highest for the acyclic **19**, and very similar for compounds **3–18**, independently from their configurations. Slightly higher values were encountered for the unsubstituted tetrahydropyran derivatives **1** and **2**. The allowable surfaces to 2 kcal/mol are very similar for the 19 compounds under study (4.9–6.8%), indicating only a minor configurational effect of the hydroxyl groups on this parameter. It was also predicted that bulky equatorial substituents vicinal to the linkage are also decreasing the flexibility.[26,30] The analysis of Table 4 indicates that HO2 has such effect in most cases: the partition functions of compounds with axial HO2 are higher or similar to those with equatorial HO2, with the exception of the pair **3**–**5**. The absolute flexibilities follow a similar trend, though an inverse effect was found when passing from compounds with D-*galacto* to those with D-*talo* configuration. The effect of HO4 is more difficult to rationalize: the partition functions of compounds with an axial HO4 have actually lower or similar values than those with an equatorial HO4, with the exception of the pair **17**–**18** (and the pair **11**–**12** when looking at the 2D partition function). On the other hand, the absolute flexibilities follow a more logical trend: an axial HO4 decreases the flexibility when HO2 is axial, whereas increases it when HO2 is equatorial. In other words, there is an increased flexibility (at least, as measured by the absolute flexibility parameter) when HO2 and HO4 carry an inverse configuration. Compounds with diaxial or diequatorial HO2–HO4 have the lower absolute flexibilities (with the exception of **18**). At last, the effect of the configuration

of HO2′ is even less noticeable. Most of the compounds show a small effect, not very systematic. The larger effects are found for compounds with D-*manno* configuration, in which an axial HO2′ increases the flexibility (measured by both q and Φ), and those with D-*talo* and D-*altro* configuration, where that configuration has an opposite effect (Table 4).

Relative Stabilities of Compounds 3–18 and Their α-Linked Counterparts

The relative steric energies of the global minimum and average energies of each compound were compared with those of their α-linked counterparts (Table 5). No major differences were found by using global minimum or average energies. As expected, compound **3**, with all equatorial substituents is the most stable. In most cases, β-linked compounds are more stable than their equivalent α-linked counterparts, but two factors act against this trend: the configurations of O2′ and O3. As expected, an axial O2′ increases the magnitude of the anomeric effect, thus augmenting the stability of the α-linked compounds. An axial O3 has a similar contribution, although of less magnitude. Thus, the highest $E_\beta - E_\alpha$ is found for compounds **3–6** (0.8–1.7 kcal/mol) with both O2′ and O3 equatorial. Intermediate values (0.1–0.7 kcal/mol) are observed for **7–14**, where one substituent is axial and the other equatorial. Finally, compounds with axial O2′ and O3 exhibit an α-anomer more stable than the β-anomer (0.1–0.5 kcal/mol). The same trend was observed when looking at free energies: in most compounds $G_\beta - G_\alpha$ is similar to $E_\beta - E_\alpha$. However, compounds with equatorial O4 (with the exception of **9** and **17**, where both O2′ and O2 are axial) have an increased $G_\beta - G_\alpha$, and **10** (axial O2 and O4) has a reduced difference.

Equatorial orientation of the hydroxyl group in cyclohexanol is favored by about 0.8 kcal/mol. As occurred for the α-linked disaccharides,[30] a similar difference is observed here (Table 5) between compounds with axial and equatorial HO4, if HO2 is also equatorial. If HO2 is axial, an axial HO4 appeared slightly favored in α-linked disaccharides.[30] Herein, with the exception of **6** (with an abnormally high energy), the same trend is observed. This is due to a strong intramolecular hydrogen-bond arrangement between the two axial groups in a 1,3-diaxial array. As expected, when observing free energies, the stabilizing effect of this diaxial array is reduced. For α-linked disaccharides, a ca. 0.8 kcal/mol effect of an axial HO2′ was encountered.[30] For β-linked disaccharides, an axial HO2′ has a much larger effect (ca. 1.6 kcal/mol), given its incidence on the anomeric effect. As occurred with α-linked disaccharides,[30] the effect of the configuration of HO2 depends on other factors: it is favorable to the equatorial position (0.9–1.6 kcal/mol) when O3 is also equatorial, negligible when O3 is axial and HO4 equatorial, and clearly favorable to the axial conformer (1.3–1.5 kcal/mol) when O3 and HO4 are axial (due to hydrogen-bonding, see above). The axial linkage on C3 always represents a large penalty, with a trend similar to that observed for α-linked compounds.[30] Equatorial HO2 and HO4 increase the magnitude of this penalty: 3.6 kcal/mol when both are equatorial, ca.1 kcal/mol when both are axial and intermediate values for the remaining cases (ca. 3 kcal/mol for equatorial HO2/axial HO4, ca.2 kcal/mol for equatorial HO4/axial HO2).

Stereochemical Consequences

^{13}C NMR glycosylation effects in disaccharides have been justified on the basis of spatial interaction of protons in different monosaccharide moieties.[30,42–44] Shashkov et al.[43] have related the different stereochemical factors (configuration of the linkage, monosaccharides, and of the carbons neighboring the linkage, chair conformation, etc.), and the experimental ^{13}C NMR glycosylation shifts. Therefore, they established the presence of two groups of disaccharides: one with a large glycosylation shift on both linked carbons, but a negligible shift on the neighboring carbons (group EII), and a second group (EI) with a smaller glycosylation shift on the linked carbons, but a substantial β-effect (ca. 3 ppm) on one of the carbons of the reducing terminus. In the present work, we have calculated the Boltzmann-averaged inter-proton distances calculated for each of the 16 disaccharides under study. The distance H1′-H3 can have two different ranges of values: 1) short (2.25–2.37 Å) for compounds with equatorial O3 and equatorial HO2 (**3**, **4**, **7** and **8**), or those with an axial O3 and an equatorial HO4 (**13**, **15** and **17**). **11** is an exception due to the high population of the **D** conformer. According to the previous rules,[43] those compounds should be gathered within group EII, with large glycosylation effects on C1′ and C3; and 2) medium (2.42–2.47 Å) for the remaining compounds, included in group EI, giving rise to smaller glycosylation effects on C1′ and C3.[43] As expected from an empirical relationship,[44] short inter-proton distances should give rise to larger glycosylation effects. In addition, the analysis of the distances of H1′ with the protons on the neighboring carbons (H2 and H4) led to the conclusion that these distances should be shorter (2.7–3.7 Å) when their corresponding hydroxyl group is axial than when it is equatorial (4.0–4.7 Å). The glycosylation effects on C1′ and C3 according to the groups EI and EII are thus probably correct in the interpretation of Shashkov et al.[43] The configuration of HO2′ is irrelevant as to the glycosylation effect or distance,[30,43] due to the strong preference for the compounds to have the ϕ angle predicted by the *exo*-anomeric effect, which shifts the ''aglycone'' apart from C2′.

ACKNOWLEDGMENTS

Both authors are Research Members of the Argentine Research Council (CONICET). This work was supported by grants from UBA (X087), CONICET and Vitae-Antorchas.

REFERENCES

1. French, A.D.; Brady, J.W. Computer modeling of carbohydrates. ACS Symp. Ser. **1990**, *430*, 1–19.
2. Engelsen, S.B.; Rasmussen, K. Conformations of disaccharides by empirical force field calculations. part v: conformational maps of β-gentiobiose in an optimized consistent force field. Int. J. Biol. Macromol. **1993**, *15* (1), 56–62.

3. French, A.D.; Dowd, M.K. Exploration of disaccharide conformations by molecular mechanics. J. Mol. Struct., Theochem **1993**, *286*, 183–201.
4. Melberg, S.; Rasmussen, K. Conformations of disaccharides by empirical force-field calculations. Part I, β-maltose. Carbohydr. Res. **1979**, *69*, 27–38.
5. Melberg, S.; Rasmussen, K. Conformations of disaccharides by empirical force-field calculations. Part II, β-cellobiose. Carbohydr. Res. **1979**, *71*, 25–34.
6. Melberg, S.; Rasmussen, K. Conformations of disaccharides by empirical, force-field calculations. Part III, β-gentiobiose. Carbohydr. Res. **1980**, *78*, 215–224.
7. Tvaroška, I.; Pérez, S. Conformational energy calculations for oligosaccharides: a comparison of methods and a strategy of calculation. Carbohydr. Res. **1986**, *149* (2), 389–410.
8. French, A.D. Rigid- and relaxed-residue conformational analyses of cellobiose using the computer program MM2. Biopolymers **1988**, *27* (9), 1519–1525.
9. Ha, S.N.; Madsen, L.J.; Brady, J.W. Conformational analysis and molecular dynamics simulations of maltose. Biopolymers **1988**, *27* (12), 1927–1952.
10. French, A.D. Comparison of rigid and relaxed conformational maps for cellobiose and maltose. Carbohydr. Res. **1989**, *188*, 206–211.
11. Tran, V.; Buléon, A.; Imberty, A.; Pérez, S. Relaxed potential energy surfaces of maltose. Biopolymers **1989**, *28*, 679–690.
12. Imberty, A.; Tran, V.; Pérez, S. Relaxed potential energy surfaces of *N*-linked oligosaccharides: the mannose-α-(1 → 3)-mannose case. J. Comput. Chem. **1989**, *11* (2), 205–216.
13. Allinger, N.L.; Yuh, Y.H.; Lii, J.-H. Molecular mechanics. The MM3 force field for hydrocarbons. J. Am. Chem. Soc. **1989**, *111* (23), 8551–8566.
14. Allinger, N.L.; Rahman, M.; Lii, J.-H. A molecular mechanics force field (MM3) for alcohols and ethers. J. Am. Chem. Soc. **1990**, *112* (23), 8293–8307.
15. Koca, J.; Pérez, S.; Imberty, A. Conformational analysis and flexibility of carbohydrates using the CICADA approach with MM3. J. Comput. Chem. **1995**, *16* (3), 296–310.
16. Koca, J. Potential energy hypersurface and molecular flexibility. J. Mol. Struct. **1993**, *291*, 255–269.
17. Dowd, M.K.; Reilly, P.J.; French, A.D. Conformational analysis of trehalose disaccharides and analogues using MM3. J. Comput. Chem. **1992**, *13* (1), 102–114.
18. Dowd, M.K.; Zeng, J.; French, A.D.; Reilly, P.J. Conformational analysis of the anomeric forms of kojibiose, nigerose, and maltose using MM3. Carbohydr. Res. **1992**, *230*, 223–244.
19. Dowd, M.K.; French, A.D.; Reilly, P.J. Molecular mechanics modeling of α-(1 → 2), α-(1 → 3), and α-(1 → 6)-linked mannosyl disaccharides with MM3(92). J. Carbohydr. Chem. **1995**, *14* (4 & 5), 589–600.
20. Dowd, M.K.; French, A.D.; Reilly, P.J. Conformational analysis of the anomeric forms of sophorose, laminaribiose, and cellobiose using MM3. Carbohydr. Res. **1992**, *233*, 15–34.
21. Stortz, C.A. Disaccharide conformational maps: how adiabatic is an adiabatic map? Carbohydr. Res. **1999**, *322*, 77–86.
22. French, A.D.; Kelterer, A.-M.; Johnson, G.P.; Dowd, M.K.; Cramer, C.J. HF/6-31G* Energy surfaces for disaccharide analogs. J. Comput. Chem. **2001**, *22* (1), 65–78.

MARCEL DEKKER, INC.
270 Madison Avenue, New York, New York 10016

23. French, A.D.; Kelterer, A.-M.; Cramer, C.J.; Johnson, G.P.; Dowd, M.K. A QM/MM analysis of the conformations of crystalline sucrose moieties. Carbohydr. Res. **2000**, *326*, 305–322.
24. French, A.D.; Kelterer, A.-M.; Johnson, G.P.; Dowd, M.K.; Cramer, C.J. Constructing and evaluating energy surfaces of crystalline disaccharides. J. Mol. Graph. Model. **2000**, *18* (2), 95–107.
25. Stortz, C.A.; Cerezo, A.S. Disaccharide conformational maps: 3D contours or 2D plots? Carbohydr. Res. **2002**, *337*, 1861–1871.
26. Rees, D.A. *Polysaccharide Shapes*; Chapman & Hall: London, 1977; 51.
27. Stortz, C.A.; Cerezo, A.S. Conformational analysis of sulfated α-(1 → 3)-linked D-galactobioses using the MM3 force-field. J. Carbohydr. Chem. **1998**, *17* (9), 1405–1419.
28. Stortz, C.A.; Cerezo, A.S. Conformational analysis of neocarrabiose and its sulfated and/or pyruvylated derivatives using the MM3 force-field. J. Carbohydr. Chem. **2000**, *19* (9), 1115–1130.
29. Stortz, C.A. Potential energy surfaces of carrageenan models: carrabiose, β-(1 → 4)-linked D-galactobiose, and their sulfated derivatives. Carbohydr. Res. **2002**, *337* (21/23), 2311–2323.
30. Stortz, C.A.; Cerezo, A.S. Potential energy surfaces of α-(1 → 3)-linked disaccharides calculated with the MM3 force-field. J. Carbohydr. Chem. **2002**, *21* (5), 355–371.
31. MM3 (96). Bull. QCPE **1997**, *17* (1), 3.
32. Engelsen, S.B.; Rasmussen, K. β-Lactose in the view of a CFF-optimized force field. J. Carbohydr. Chem. **1997**, *16* (6), 773–788.
33. Takeda, H.; Yasuoka, N.; Kasai, N. The crystal and molecular structure of a 3:2 mixture of laminarabiose and *O*-α-D-glucopyranosyl-(1 → 3)-β-D-glucopyranose. Carbohydr. Res. **1977**, *53*, 137–152.
34. Takeda, H.; Kaiya, T.; Yasuoka, N.; Kasai, N. The crystal and molecular structure of methyl 2,4,6-tri-*O*-acetyl-3-*O*-(2,3,4,6-tetra-*O*-acetyl-β-D-glucopyranosyl)-β-D-glucopyranoside (methyl 2,3,4,6,2′,4′,6′-hepta-*O*-acetyl-β-D-laminarabioside). Carbohydr. Res. **1978**, *62*, 27–37.
35. Perez, S.; Vergelati, C.; Tran, V.H. Real-space crystal structure solution. Crystal and molecular structure of laminarabiose octaacetate, $C_{28}H_{38}O_{19}$. Acta Crystallogr., Sect. B **1985**, *41*, 262–275.
36. Noguchi, K.; Okuyama, K.; Kitamura, S.; Takeo, K. Crystal structure of methyl 3-*O*-β-D-glucopyranosyl-β-D-glucopyranoside (methyl β-D-laminarabioside) monohydrate. Carbohydr. Res. **1992**, *237*, 33–43.
37. Ikegami, M.; Noguchi, K.; Okuyama, K.; Kitamura, S.; Takeo, K.; Ohno, S. Molecular and crystal structure of methyl hepta-*O*-acetyl-α-laminarabioside. Carbohydr. Res. **1994**, *253*, 29–38.
38. Noguchi, K.; Kobayashi, E.; Okuyama, K.; Kitamura, S.; Takeo, K.; Ohno, S. Molecular and crystal structure of (2,3,4,6-tetra-*O*-acetyl-β-D-glucopyranosyl)-(1 → 3)-[2,3,4,6-tetra-*O*-acetyl-β-D-glucopyranosyl-(1 → 6)-(2,4-di-*O*-acetyl-β-D-glucopyranosyl)-(1 → 3)-1,2,4,6-tetra-*O*-acetyl-β-D-glucopyranose. Carbohydr. Res. **1994**, *258*, 35–47.
39. Foces-Foces, C.; Cano, F.H.; García-Blanco, S. 1,2,4,6-Tetra-*O*-acetyl-3-*O*-(2,3,4,6-tetra-*O*-acetyl-β-D-galactopyranosyl)-α-D-galactopyranose. Acta Crystallogr., Sect. B **1980**, *36*, 377–384.

Marcel Dekker, Inc.
270 Madison Avenue, New York, New York 10016

40. Mendonca, S.; Johnson, G.P.; French, A.D.; Laine, R.A. Conformational analyses of native and permethylated disaccharides. J. Chem. Phys. A **2002**, *106*, 4115–4124.
41. Rees, D.A.; Scott, W.E. Polysaccharide conformation. Part VI. Computer model-building for linear and branched pyranoglycans. Correlations with biological function. Preliminary assessment of inter-residue forces in aqueous solution. Further interpretation of optical rotation in terms of chain conformation. J. Chem. Soc., B **1971**, 469–479.
42. Kochetkov, N.K.; Chizhov, O.S.; Shashkov, A.S. Dependence of ^{13}C chemical shifts on the spatial interaction of protons, and its application in structural and conformational studies of oligo- and polysaccharides. Carbohydr. Res. **1984**, *133*, 173–185.
43. Shashkov, A.S.; Lipkind, G.M.; Knirel, Yu.A.; Kochetkov, N.K. Stereochemical factors determining the effects of glycosylation on the ^{13}C chemical shifts in carbohydrates. Magn. Reson. Chem. **1988**, *26*, 735–747.
44. Bock, K.; Brignole, A.; Sigurskjold, B.W. Conformational dependence of ^{13}C nuclear magnetic resonance chemical shifts in oligosaccharides. J. Chem. Soc., Perkin Trans. 2 **1986**, 1711–1713.

Received October 10, 2002
Accepted February 3, 2003

MARCEL DEKKER, INC.
270 Madison Avenue, New York, New York 10016